A multivalent inhibitor of the DC-SIGN dependent uptake of HIV-1 and Dengue virus

Norbert Varga,[1§] Ieva Sutkeviciute,[2,3,4§] Renato Ribeiro-Viana,[5§] Angela Berzi[6], Rasika Ramdasi,[7] Anna Daghetti, [1] Gerolamo Vettoretti, [1] Ali Amara,[7] Mario Clerici,[8,9] Javier Rojo,*[5] Franck Fieschi,*[2,3,4] Anna Bernardi*[1,10]

1. Universita' degli Studi di Milano, Dipartimento di Chimica, via Golgi 19, 20133 Milano, Italy; 2. Univ. Grenoble Alpes, Institut de Biologie Structurale (IBS), F-38027 Grenoble, France ; 3. CEA, DSV, IBS, F-38027 Grenoble, France; 4. CNRS, IBS, F-38027 Grenoble, France; 5. Instituto de Investigaciones Químicas (IIQ), CSIC – Universidad de Sevilla, Americo Vespucio 49, 41092 Sevilla, Spain; 6. Università degli Studi di Milano, Dipartimento di Scienze Biomediche e Cliniche "L. Sacco", Via GB Grassi 74, 20157 Milano, Italy; 7. INSERM U944, Laboratoire de Pathologie et Virologie Moléculaire, Hôpital Saint-Louis, 1 Avenue Claude Vellefaux, 75010 Paris, France; 8. Università degli Studi di Milano, Dipartimento di Fisiopatologia Medico-chirurgica e dei Trapianti, Via F.lli Cervi 93, 20090 Segrate, Italy; 9. Fondazione Don Gnocchi IRCCS, Via Capecelatro 66, 20148 Milano, Italy; 10. CNR-ISTM, Institute of Molecular Science and Technologies, Milan, Italy

§ These authors contributed equally to this paper

Keywords: Glycodendrimers, Glycomimetics, HIV, Dengue, DC-SIGN, Nanotechnology

Abstract

DC-SIGN is a C-type lectin receptor on antigen presenting cells (dendritic cells) which has an important role in some viral infection, notably by HIV and Dengue virus (DV). Multivalent presentation of carbohydrates on dendrimeric scaffolds has been shown to inhibit DC-SIGN binding to HIV envelope glycoprotein gp120, thus blocking viral entry. This approach has interesting potential applications for infection prophylaxis. In an effort to develop high affinity inhibitors of DC-SIGN mediated viral entry, we have synthesized a group of glycodendrimers of different valency that bear different carbohydrates or glycomimetic DC-SIGN ligands and have studied their DC-SIGN binding activity and antiviral properties both in an HIV and a Dengue infection model. Surface Plasmon Resonance (SPR) competition studies have demonstrated that the materials obtained bind efficiently to DC-SIGN with IC_{50}s in the μM range, which depend on the nature of the ligand and on the valency of the scaffold. In particular, a hexavalent presentation of the DC-SIGN selective antagonist **4** displayed high potency, as well as improved accessibility and chemical stability relative to previously reported dendrimers. At low μM concentration the material was shown to block both DC-SIGN mediated uptake of DV by Raji cells and HIV *trans*-infection of T-cells.

Introduction

Cells of the innate immune system use pattern recognition receptors (PRRs) to identify pathogen-associated molecular patterns. The two major families of membrane-bound PRRs found in sentinel cells, as macrophages and dendritic cells, are Toll-like receptors (TLRs) and C-type lectin receptors (CLRs). DC-SIGN (Dendritic Cell-Specific Intercellular adhesion molecule-3-Grabbing Nonintegrin) is a CLR used by immature dendritic cells (DCs) in mucosal tissue to recognize high-mannose glycans present on the surface of invading microorganisms. For some pathogens, including viruses like HIV, Ebola or Dengue,[1] this recognition event contributes to infection by promoting viral transmission, rather than protecting the host. This observation has turned DC-SIGN into an interesting target for the design of anti-viral agents.[2-10] The task is complicated by the presence of other C-type lectins of similar selectivity, like Langerin,[11] that has a protective effect against HIV infection. Thus, selective DC-SIGN ligands that interact only weakly with Langerin are actively sought after as potentially useful therapeutic tools against HIV and other viruses that use DC-SIGN as a primary receptor.[12-15]

DC-SIGN is a tetramer and is organized into clustered patches at the cell membrane.[16, 17] Interactions with pathogens, also expressing multiple copies of clustered glycans, involve a complex equilibrium that implies multipoint attachments. For this reason the principle of multivalency has been used with success in the development of antagonists of DC-SIGN and numerous reports have appeared in the literature concerning mannosylated dendrimers or polymers that target it.[8, 10, 18-22] Multivalent structures bearing sugar mimics were previously prepared in our group[10, 18] using Boltorn type dendrimers and dendrons derived from 2,2-bis(hydroxymethyl) propionic acid. These scaffolds have a polyester backbone of good flexibility and water solubility, and their outer layers are functionalized with carboxylic groups. Ligand conjugation occurs *via* amide bond formation with amine functionalities on the monovalent ligands. In particular, the tetravalent pseudo-trimannoside **1.2** (Figure 1), bearing four copies of the trimannoside mimic **2a**, was found to interact selectively with DC-SIGN versus Langerin and block

HIV-1 infection both in cellular and human cervical explant models.[12, 13] Further analysis of multivalent constructs bearing up to 30-32 copies of trimannoside mimic **2a** or the corresponding pseudo-disaccharide **3a**[18] provided nanomolar inhibitors of an Ebola pseudotyped virus infection, but showed some drawbacks, such as relatively long synthesis and chemical instability of the scaffolds. Additionally, these studies revealed that the pseudo-disaccharide **3**, once presented on a polyvalent construct, is only marginally less active as a DC-SIGN antagonist than the more synthetically complex pseudo-trisaccharide **2**. Further campaigns, directed to optimization of the pseudo-disaccharide structure, led to a new lead, the bis-benzylamide **4**, which binds DC-SIGN with an affinity approaching that measured for **2,** while displaying improved selectivity.[15]

In the development of this research, we have sought to exploit antagonist **4** as the active element of new glycodendrimers. To overcome the problems met with Boltorn-type structures, a set of polyalkynes were planned as dendrimer cores, in order to take advantage of Cu(I) catalyzed azide-alkyne cycloaddition (CuAAC, click chemistry) of **4**. This approach has the potential to afford multivalent DC-SIGN antagonists of high potency, that also display improved accessibility and chemical stability over previously studied materials. Their DC-SIGN binding properties could be studied in Surface Plasmon Resonance (SPR) and in infection cellular models, using azido-functionalized mannose **5**[23], the pseudo-trisaccharide **2b**[24] and pseudo-disaccharide **3b**[25] to synthesize appropriate controls.

2. Materials and methods

2.1 Synthesis

2.1.1 General

Dichloromethane, methanol, N,N-diisopropylethylamine and triethylamine were dried over calcium hydride; THF was distilled over sodium, N,N-dimethylacetamide (DMA) was dried over activated molecular sieves (4 Å). Reactions requiring anhydrous conditions were performed under nitrogen. ^{1}H and ^{13}C spectra were recorded at 500 MHz on a Bruker DRX 500, 400 MHz on a Bruker

AVANCE-400 and 300 MHz on Bruker DPX-300 instrument. Chemical shifts (δ) for ^{1}H and ^{13}C spectra are expressed in ppm relative to internal standard ($CDCl_3$: 7.24 for ^{1}H and 77.23 for ^{13}C; CD_3OD: 3.31 for ^{1}H and 49.15 for ^{13}C; D_2O: 4.80 for ^{1}H; DMSO-D_6: 2.50 for ^{1}H and 39.52 for ^{13}C). Signals were abbreviated as s, singlet; br s, broad singlet; d, doublet; t, triplet; q, quartet; m, multiplet. Mass spectra were obtained with a ThermoFisher LCQ apparatus (ESI ionization), or iontrap ESI Esquire 6000 from Bruker, or a Microflex apparatus (MALDI ionization) from Bruker, or Apex II ICR FTMS (ESI ionization-HRMS). Specific optical rotation values were measured using a Perkin-Elmer 241, at 589 nm, in a 1 dm cell. Thin layer chromatography (TLC) was carried out with pre-coated Merck F254 silica gel plates. Flash chromatography (FC) was carried out with Macherey-Nagel silica gel 60 (230–400 mesh).

Compounds **3**, [25] **4,** [15] **7,** [26] **9,** [27] **11,** [28] and **14**[29] have been previously described. The tetravalent mannosylated dendrimer **11.5** is a known compound.[28] The synthesis and characterization of materials derived from monovalent ligand **4** (**11.4**, **13.4** and **9.15.4**) is described below. The synthesis and characterization of all other glycodendrimers are reported in the Supplementary Information file.

The numbering used in the NMR characterizations is indicated in the structures reported in the Supplementary Information file (Figure SI-9). Sugar signals were numbered as customary; cyclohexane protons are indicated with the letter D followed by numbers. The unusual numbering of the pseudo-saccharide derivatives in the NMR characterizations was adopted to facilitate comparison with the native disaccharide

2.1.2 General procedure for the CuAAC reaction (click reactions)

In the optimized procedure of the copper(I) catalyzed 1,3-dipolar cycloaddition, the starting materials and reagents were added to the reaction mixtures as solutions in water (degased by bubbling with nitrogen) or THF (freshly distilled). Monovalent ligands (**2-4**) and dendrons (**15.3** and **15.4**) with azide groups were added as solids. The reagents were added to the reaction in the following order: multivalent scaffold (1 eq. in THF), TBTA (1 eq. in THF), copper(II) sulphate

(0.1 eq. in H_2O), sodium ascorbate (0.4 eq. in H_2O) and finally the azide derivative (1.1 eq. per alkyne). After the addition of all the reagents, the solvent ratio was adjusted to 1:1 by addition of THF and/or water (c = ~ 0.03 M). The reactions were stirred under nitrogen atmosphere, and protected from light. The reaction progress was followed by TLC (silica, Hex:EtOAc = 8:2 and C18, H_2O: MeOH = 1:1) or mass spectrometry (MALDI or ESI ionization). Usually, in order to achieve reaction completion, an additional 0.4 eq. of sodium ascorbate was added (2-4 h after reaction start). After reaction completion the mixtures were loaded directly on SEPHADEX LH-20 columns (55 cm x 3.5 cm, MeOH as eluent) to purify the products by size exclusion chromatography. In order to remove copper residues from the products, reverse phase chromatography was performed (C18, eluent: H_2O with gradients of MeOH or MeCN) or to the solution of product in MeOH a metal scavenger[30] (such as Quadrasil^{TM} MP) was added and stirred for 5 min. The scavenger was filtered off through a cotton pad and the filtrate was concentrated to obtain the product.

2.1.3 Synthesis of hexa(2-propynyloxymethyl) bispentaerythritol, 13

To a solution of bispentaerythritol (0.3 g, 1.18 mmol, 1 eq.) in dry DMF (20 mL), sodium hydride (0.34 g, 14 mmol, 11.8 eq.) was added under argon at -5ºC. The solution was stirred at -5ºC for 1 h then propargyl bromide (1.15 mL, 14 mmol, 11.8 eq.) was added and the mixture was kept at -5ºC for additional 20 min. The reaction was let to warm up to room temperature and stirred for 19 h. The reaction was cooled to 0ºC, quenched by slow addition of water and extracted with diethyl ether (3 x 30 mL). The combined organic phases were dried over sodium sulphate and concentrated under reduced pressure. The crude was purified by flash chromatography (silica, hex:Ethyl Acetate = 9:1 and 8.5:1.5) to afford 130 mg of pure product. **Yield:** 65%; **MS (HRMS)** calculated for $[C_{28}H_{34}O_7Na]^+$: 483.2383; found = 483.2379; **^{1}H NMR** (300 MHz, $CDCl_3$): δ = 4.12 (d, 12H, H_3, $J_{3\text{-}1}$ = 2.4 Hz), 3.52 (s, 12H, H_4), 3.38 (s, 4H, H_6), 2.53 (t, 6H, H_1, $J_{3\text{-}1}$ = 2.4 Hz); **^{13}C NMR** (75 MHz, $CDCl_3$): δ = δ 80.2 (C_1); 74.3 (C_2); 69.9 (C_3); 69.3 (C_4); 58.9 (C_6); 45.2 (C_5).

*2.1.4 Synthesis of tetravalent glycodendrimer **11.4***

Prepared according to the general procedure starting from **11**[28] and **4**[15]. **Reaction time:** 18 h; **Yield:** 87%; $[\alpha]_D^{25}$ = - 4.7 (c = 0.21, MeOH); **MS (MALDI, matrix: α-cyano-4-hydroxy-cinnamic acid, solvent: MeOH):** calculated for $[C_{145}H_{192}N_{20}O_{48}Na]^+$: 3006.2; found = 3005.4; **MS (ESI-HRMS):** calculated for $[C_{145}H_{192}N_{20}O_{48}]^+$: 2981.3198; found = 2981.3244 (after deconvolution, error: 1.6 ppm); **^{1}H NMR** (400 MHz, CD_3OD): δ = 7.96 (s, 4H, H_{16}), 7.31 – 7.07 (m, 32H, H_{12}, H_{13}), 4.89 (br s, 4H, H_1), 4.54 (s, 16H, H_{15}), 4.51 (t, 8H, H_8, $J_{8\text{-}7}$ = 5.4 Hz), 4.44 (s, 8H, H_{18}), 4.27 (s, 8H, H_{10a}), 4.25 (s, 8H, H_{10b}), 3.95 - 3.80 (m, 20H, H_2, H_{6a}, D_2, H_7), 3.72 - 3.60 (m, 12H, H_{6b}, D_1, H_3), 3.59 - 3.49 (m, 8H, H_4, H_5), 3.44 (br s, 8H, H_{19}), 2.90 – 2.75 (m, 8H, D_4, D_5), 1.96 – 1.66 (m, 16H, D_3, D_6); **^{13}C NMR** (100 MHz, CD_3OD): δ = 177.1, 176.9 (C_9); 146.3 (C_{17}); 141.7 (C_{14}); 139.2 (C_{11}); 128.5, 128.3 (C_{13}, C_{12}); 126.2 (C_{16}); 100.6 (C_1); 76.3 (C_3); 75.7 (C_{D1}); 72.7 (D_2); 72.5 (C_2); 72.4 (C_5); 70.0 (C_{19}); 69.0 (C_4); 68.5 (C_7); 65.5 (C_{18}); 65.1 (C_{15}); 63.3 (C_6); 52.6 (C_{10}); 51.7 (C_8); 46.7 (C_{20}); 43.8 (C_{10}); 41.9, 41.9 (C_{D4}, C_{D5}); 29.9, 29.2 (C_{D3}, C_{D6}).

*2.1.5 Synthesis of hexavalent glycodendrimer **13.4***

Prepared according to the general procedure starting from **13** and **4**[15]. **Reaction time:** 18 h; **Yield:** 70%; $[\alpha]_D^{25}$ = - 2.8 (c = 0.27, MeOH); **MS (MALDI, matrix: 2,5-dihydroxybenzoic acid, solvent: MeOH)**; calculated for $[C_{220}H_{292}N_{30}O_{73}]^+$: 4524.8; found = 4524.7 $[M]^+$ and 4549.1$[M+Na]^+$; **MS (ESI-HRMS)**: calculated for $[C_{220}H_{292}N_{30}O_{73}]^+$: 4522.0059; found = 4522.0147 (after deconvolution, error: 2.0 ppm); **^{1}H NMR** (400 MHz, CD_3OD): δ = 7.95 (s, 6H, H_{16}), 7.28 – 7.07 (m, 48H, H_{12}, H_{13}), 4.89 (br s, 6H, H_1), 4.54 (s, 24H, H_{15}), 4.51 - 4.45 (m, 12H, H_8), 4.44 (s, 12H, H_{18}), 4.28 - 4.20 (m, 24H, H_{10}), 3.95 - 3.80 (m, 30H, H_2, H_{6a}, D_2, H_7), 3.73 - 3.61 (m, 18H, H_{6b}, D_1, H_3), 3.60 - 3.47 (m, 12H, H_4, H_5), 3.38 (br s, 12H, H_{19}), 3.26 (br s, 4H, H_{21}), 2.89 – 2.78 (m, 12H, D_4, D_5), 1.93 – 1.69 (m, 24H, D_3, D_6); **^{13}C NMR** (100 MHz, CD_3OD): δ = 177.1, 176.9 (C_9); 146.3 (C_{17}); 141.7 (C_{14}); 139.2 (C_{11}); 128.6, 128.3 (C_{13}, C_{12}); 126.1 (C_{16}); 100.7 (C_1); 76.3 (C_3); 75.7 (C_{D1}); 72.7 (D_2); 72.5 (C_2, C_5); 71.1 (C_{21}); 70.3 (C_{19}); 69.0 (C_4); 68.5 (C_7); 65.5

(C_{18}); 65.1 (C_{15}); 63.3 (C_6); 52.6 (C_{10}); 51.7 (C_8); 43.8 (C_{10}); 41.9, 41.9 (C_{D4}, C_{D5}); 29.9, 29.3 (C_{D3}, C_{D6}).

*2.1.6 Synthesis of trivalent glycodendron **15.4***

Dendron **14.4** was initially prepared, according to the general procedure and starting from **14**[29] and **4**[15]. **Reaction time:** 3 h; **Yield:** 81%; **MS (MALDI matrix: sinapinic acid, solvent: MeOH)**: calculated for $[C_{114}H_{154}ClN_{15}O_{38}]^+$: 2378.0; found = 2378.5; **^{1}H NMR** (400 MHz, CD_3OD): δ = 7.98 (s, 3H, H_{16}); 7.28 – 7.16 (m, 24H, H_{12}, H_{13}); 4.89 (br s, 3H, H_1); 4.58 – 4.50 (m, 6H, H_8); 4.55 (s, 12H, H_{15}); 4.48 (s, 6H, H_{18}); 4.28 (s, 6H, H_{10}); 4.26 (s, 6H, H_{10}); 3.99 - 3.80 (m, 15H, H_2, H_{6a}, D_2, H_7); 3.73 - 3.61 (m, 11H, H_{6b}, D_1, H_3, H_{25}); 3.61 - 3.44 (m, 12H, H_4, H_5, H_{22}, H_{23}, H_{24}), 3.42 (br s, 6H, H_{19}), 3.39 (br s, 2H, H_{21}), 2.90 – 2.76 (m, 6H, D_4, D_5), 1.96 – 1.68 (m, 12H, D_3, D_6); **^{13}C NMR** (100 MHz, CD_3OD): δ = 177.1, 176.9 (C_9), 146.3 (C_{17}), 141.7 (C_{14}), 139.2 (C_{11}), 128.5, 128.3 (C_{13}, C_{12}), 126.2 (C_{16}), 100.5 (C_1), 76.3 (C_3); 75.7 (C_{D1}); 72.7 (D_2); 72.6 (C_{24}); 72.5, 72.4 (C_2, C_5); 72.2, 71.5 (C_{22}, C_{23}); 70.9 (C_{21}); 70.2 (C_{19}); 69.0 (C_4); 68.5 (C_7); 65.5 (C_{18}); 65.1 (C_{15}); 63.3 (C_6); 51.7 (C_8); 46.7 (C_{20}); 44.2 (C_{25}); 43.8 (C_{10}); 41.9, 41.9 (C_{D4}, C_{D5}); 29.9, 29.3 (C_{D3}, C_{D6}).

To a solution of **14.4** (150 mg, 0.0631 mmol, 1 eq.) in DMF (1 mL) sodium azide (25 mg, 0.378 mmol, 6 eq.) was added. The reaction was stirred at 65ºC for 4 days. The solvent was removed under reduced pressure and the resulting crude was purified by reverse phase flash chromatography (C18, water with gradient of MeOH from 0% to 70%) to afford 143 mg of pure product. **Yield:** 95%; **MS (MALDI matrix: sinapinic acid, solvent: MeOH)**: calculated for $[C_{114}H_{154}N_{18}O_{38}]^+$: 2384,5; found = 2385.3; **^{1}H NMR** (400 MHz, CD_3OD): δ = 7.98 (s, 3H, H_{16}), 7.30 – 7.13 (m, 24H, H_{12}, H_{13}), 4.89 (br s, 3H, H_1), 4.60 – 4.50 (m, 6H, H_8), 4.55 (s, 12H, H_{15}), 4.48 (s, 6H, H_{18}), 4.28 (s, 6H, H_{10}), 4.26 (s, 6H, H_{10}), 3.97 - 3.80 (m, 15H, H_2, H_{6a}, D_2, H_7), 3.73 - 3.62 (m, 9H, H_{6b}, D_1, H_3), 3.62 - 3.46 (m, 14H, H_4, H_5, H_{22}, H_{23}, H_{24}, H_{25}), 3.43 (br s, 6H, H_{19}), 3.40 (br s, 2H, H_{21}), 2.90 – 2.76 (m, 6H, D_4, D_5), 1.96 – 1.69 (m, 12H, D_3, D_6).; **^{13}C NMR** (100 MHz,

CD_3OD): δ = 177.1, 176.8 (C_9), 146.3 (C_{17}), 141.7 (C_{14}), 139.2 (C_{11}), 128.5, 128.3 (C_{13}, C_{12}), 126.2 (C_{16}), 100.5 (C_1), 76.3 (C_3); 75.7 (C_{D1}); 72.7 (D_2); 72.5, 72.4 (C_2, C_5); 72.3, 71.5, 71.3 (C_{22}, C_{23}, C_{24}); 70.9 (C_{21}); 70.2 (C_{19}); 69.0 (C_4); 68.5 (C_7); 65.5 (C_{18}); 65.1 (C_{15}); 63.2 (C_6); 51.9 (C_{25}); 51.7 (C_8); 46.7 (C_{20}); 43.8 (C_{10}); 41.9, 41.8 (C_{D4}, C_{D5}); 29.9, 29.2 (C_{D3}, C_{D6}).

*2.1.7 Synthesis of nonavalent glycodendrimer **9.15.4***

Prepared according to the general procedure starting from **9**[27] and **15.4**. **Reaction time:** 18 h; **Yield:** 75%; **MS (MALDI, matrix: sinapinic acid, solvent: MeOH)**: calculated for $[C_{357}H_{474}N_{54}O_{117}]^+$: 7393,9; found = 7394.5; **MS (ESI-HRMS)**: calculated for $[C_{357}H_{474}N_{54}O_{117}]^+$: 7389.2801; found = 7393.2866 (after deconvolution, error: 0.7 ppm); **^{1}H NMR** (400 MHz, CD_3OD): δ = 8.05 (s, 3H, H_{26}), 7.95 (s, 9H, H_{16}), 7.28 – 7.11 (m, 72H, H_{12}, H_{13}), 6.29 (br s, 3H, H_{30}), 5.03 (br s, 6H, H_{28}), 4.89 (br s, 9H, H_1), 4.63 (s, 6H, H_{25}), 4.55 (s, 36H, H_{15}), 4.52 – 4.46 (m, 18H, H_8), 4.45 (s, 12H, H_{18}), 4.27 (s, 18H, H_{10}), 4.25 (s, 18H, H_{10}), 3.96 - 3.75 (m, 51H, H_2, H_{6a}, D_2, H_7, H_{24}), 3.75 - 3.62 (m, 27H, H_{6b}, D_1, H_3), 3.61 - 3.42 (m, 30H, H_4, H_5, H_{22}, H_{23}), 3.39 (br s, 18H, H_{19}), 3.36 (br s, 6H, H_{21}), 2.89 – 2.81 (m, 18H, D_4, D_5), 1.96 – 1.68 (m, 36H, D_3, D_6).

^{1}H NMR (400 MHz, DMSO-D_6): δ = 8.31 (t, 9H, H_{NH}, $J_{10\text{-}NH}$ = 5.3 Hz), 8.31 (t, 9H, H_{NH}, $J_{10\text{-}NH}$ = 5.3 Hz), 8.17 (s, 3H, H_{26}), 8.01 (s, 9H, H_{16}), 7.24 – 7.07 (m, 72H, H_{12}, H_{13}), 6.33 (br s, 3H, H_{30}), 5.09 (t, 18H, $H_{OH\text{-}C15}$, $J_{H15\text{-}OH}$ = 5.6 Hz), 5.05 (br s, 6H, H_{28}), 4.76 (br s, 9H, H_1), 4.74 (d, 9H, $H_{OH\text{-}C3}$, $J_{H3\text{-}OH}$ = 4.6 Hz), 4.67 (d, 9H, $H_{OH\text{-}C2}$, $J_{H2\text{-}OH}$ = 3.9 Hz), 4.59 (d, 9H, $H_{OH\text{-}C4}$, $J_{H4\text{-}OH}$ = 5.5 Hz), 4.54 – 4.46 (m, 27H, H_8, $H_{OH\text{-}C4}$), 4.46 - 4.37 (m, 54H, H_{15}, H_{18}), 4.17 (br s, 36H, H_{10}), 3.93 - 3.85 (m, 9H, H_{7a}), 3.83 – 3.72 (m, 18H, D_2, H_{7b}), 3.72 – 3.62 (m, 18H, H_2, H_{6a}), 3.60 (br s, 9H, D_1), 3.52 - 3.20 (m, 84H, H_3, H_4, H_5, H_{6b}, H_{19}, H_{21}, H_{22}, H_{23}, H_{24}, H_{25}), 2.81 – 2.63 (m, 18H, D_4, D_5), 1.83 – 1.46 (m, 36H, D_3, D_6).**^{13}C NMR** (100 MHz, DMSO-D_6): δ = 174.1, 174.0 (C_9); 144.0 (C_{29}); 140.7 (C_{14}); 138.0 (C_{11}); 126.7, 126.6, 126.3 (C_{12} ,C_{13}); 124.9 (C_{26}); 124.2 (C_{16}); 98.8 (C_1); 94.5 (C_{30}); 74.6 (C_5); 74.2 (C_{D1}); 70.9 (C_3); 70.5 (C_2); 70.4 (D_2); 69.1 (C_{21}); 68.7 (C_{19}); 67.1 (C_7); 67 - 63 (C_{22},

C_{23}, C_{24}); 62.7 ($C_{15,}$ C_{18}); 61.3 ($C_{28,}$ C_6); 49.4 (C_8); 44.9 (C_{25}); 41.6 (C_{10}); 39.3 (C_{D4}, C_{D5}); 28.2, 27.9 (C_{D3}, C_{D6}).

2.2 SPR methods.

SPR competition experiments were performed on a Biacore 3000 instrument. Flow cells (Fc) 2 and 1 of sensor chip CM4 were functionalized with mannosylated bovine serum albumine (Man α1-3[Manα1-6]Man BSA (Man-BSA), Dextra Laboratories) or prepared as control surface, respectively, as described previously[15]. The final response of immobilized Man-BSA was 5000 RU.

The competition experiment was performed using 25 mM Tris-HCl pH 8, 150 mM NaCl, 4 mM $CaCl_2$, 0.005% P20 as the running buffer at 5 μL/min flow rate. The binding of soluble tetrameric DC-SIGN ECD [31]to immobilized Man-BSA was inhibited by the compounds at increasing concentrations (0.14 μM – 900 μM for multivalent compounds, and 0.69 μM – 4.5 mM for monovalent ligands). For this reason, 13 μL of each DC-SIGN ECD (24 μM)/compound mixture was injected over the surfaces. The bound lectin was washed off by a 1 min injection of 50 mM EDTA pH 8. DC-SIGN ECD equilibrium binding responses (R_{eq}) for each sample were obtained from the reference surface corrected sensorgrams 150 s after the start of the injection.

$$y = R_{hi} - \frac{R_{hi} - R_{lo}}{1 + \left(\frac{Conc}{A_1} \right)^{A_2}} \quad (1)$$

$$IC_{50} = A_1 \cdot \left(\frac{R_{hi} - R_{lo}}{R_{hi} - 50} - 1 \right)^{\frac{1}{A_2}} \quad (2)$$

where R_{hi} and R_{lo} are maximum and minimum asymptotes, A_1 is an inflection point and A_2 is a slope of the curve.

The obtained R_{eq} values were converted to DC-SIGN residual activity values (y, %) with respect to R_{eq} of DC-SIGN alone, which was assigned a 100% activity value. After plotting residual activity

against corresponding compound concentration, the 4-parameter logistic model (eq, 1) was fitted to the plots, and finally the IC_{50} values were calculated using equation 2.

2.3 Infection studies methods

2.3.1 HIV infection studies.

For HIV studies, B-THP-1/DC-SIGN cells, that support DC-SIGN mediated HIV-1 transmission efficiently, were exploited as a model of DCs. Non-transfected B-THP-1 cells were used as a negative control. B-THP-1/DC-SIGN cells[32] or B-THP-1 cells were pre-incubated for 30 minutes in the presence or absence of the DC-SIGN inhibitors and afterwards were pulsed with HIV (the R5 tropic laboratory-adapted strain HIV-1 BaL) in the continued presence of inhibitors. After washing, B-THP-1/DC-SIGN cells were co-cultured with activated CD4+ T lymphocytes from healthy volunteer donors. To monitor viral infection of CD4+ T lymphocytes, HIV-1 p24 concentration in the co-culture supernatants was assessed by ELISA. Each point was obtained in triplicate using CD4+ T lymphocytes derived from three different healthy donors, and each compound was tested at three different concentrations (1 μM, 10 μM and 100 μM). Details are given in the Supplementary information.

2.3.2 DV infection studies.

Raji cells over-expressing DC-SIGN were infected with Dengue virus serotype-2 in the presence or absence of **13.4** at three different concentrations (10 μM, 5 μM and 1 μM). The infection was scored after 48 hours at 37°C, using DV prM protein specific antibody 2H2. Mannan at 250 μg/mL was used as positive control for infection inhibition.

2.3.3 Cyotoxicity studies

To assess the potential cytotoxicity of the glycodendrimers tested in cellular models (**11.3**, **11.4**, and **13.4**), B-THP-1/DC-SIGN cells or pheripheral blood mononuclear cells (PBMCs) were incubated for the indicated time intervals with different concentrations of the compounds (1 μM, 10 μM, and 100 μM), followed by staining with 7-aminoactinomicin D (7-AAD), that penetrates cell membrane of dying or dead cells. Percentage of 7-AAD positive cells (non-viable cells) did not change

significantly in the absence of the compounds or in their presence up to 100 μM, the highest concentration assayed in the cellular infection models (Supplementary **Figures SI-4** and **SI-5**).

The cytotoxicity of **13.4** towards Raji-DC-SIGN cells was also assessed using the MTT test (Figure SI-6, MTT cytotoxicity testing kit from Sigma). The experiment was performed according to manufacturer's instructions. Different concentrations of **13.4** were tested on Raji-DC-SIGN cells and percentage of live cells was directly proportional to the absorbance detected by spectrophotometer. The absorbance values were expressed as relative percentage compared to mock cells. Equal amount of DMSO was used as control. The results indicate that **13.4** is not cytotoxic to cells at the concentrations used in the infection assays.

3. Results and discussion.

3.1 Synthesis and characterization of the glycodendrimers

The divalent alkyne **7**[26] was prepared from ditosylate **6** by reaction with an excess of propargyl alcohol in the presence of potassium carbonate (Scheme 1)**.** Compounds **9**, [27] **11,** [27] and **13** were prepared in one step from commercially available starting materials. The general strategy is based on treating polyalcohols **8**, **10** or **12** with an appropriate base in the presence of propargyl bromide (Scheme 1). The basic structures **7**, **9**, **11**, **13** can lead to di-, tri-, tetra- and hexa-valent presentations of a monovalent ligand, respectively. Additionally, the known trivalent dendron **14** [29] was prepared from **10** (Scheme 1). Dendron **14** can be functionalized by Cu(I) catalyzed azide-alkyne cycloaddition (CuAAC) with three copies of a ligand and, after transformation of the chloride tethered to the focal point into an azide (yielding **15**, Figure 2), it can be clicked on other polyalkynes such as **7**, **9**, **11**, **13**, leading to compounds with higher valency and different shapes (Figure 2).

With this approach the 17 polyvalent constructs shown in Figure 2 were synthesized by CuAAC with ligands **2b**, **3b**, **4-5**. Among them, one tetravalent (**11.4**), one hexavalent (**13.4**) and one nonavalent (**9.15.4**) dendrimers bear the lead mimic **4** (Figure 2)**.** Controls with valency up to 18

were built using mannose **5**, the pseudo-dimannoside **3** and the pseudo-trimannoside **2** as the monovalent ligand (see Supplementary Information). The dendrimers were isolated from the reaction mixtures by size exclusion chromatography on Sephadex LH20 matrix using MeOH as eluent. Residual copper was removed either by reverse phase chromatography (C18) or using metal scavengers (Quadrasil MP)[30]. All materials were found to be stable for months in water solution and were fully characterized by MALDI-MS analysis (sinapinic acid or DBA) and by ^{1}H and ^{13}C-NMR spectroscopy.

3.2 Surface Plasmon Resonance studies

All the glycodendrimers were tested by SPR, using a protocol that we have previously described.[33] The assay allows to compare the relative affinity of ligands on the basis of their ability to inhibit DC-SIGN binding to mannosylated bovine serum albumin (Man-BSA) immobilized onto a carboxymethyl dextran- functionalized gold SPR sensor chip (CM4). Inhibition studies were performed using the extracellular domain (ECD) of DC- SIGN (24 μM) injected alone or in the presence of increasing concentrations of ligands. The 50% inhibition concentration (IC_{50}) of the dendrimers was determined and the values were compared to those obtained with the previously described tetravalent Boltorn-type dendrons **1.**

Figure 3 shows the results of a first series of experiments focused on materials derived from the pseudo-disaccharide **3.** This set of experiments revealed that the pentaerythritol based dendrimers compare well with the previously studied Boltorn-type ones. Indeed, the two tetravalent presentations **1.3** and **11.3** display basically the same activity and the same relative inhibitory potency (RIP) per ligand unit (ca. 1.5) compared to the monovalent counterpart **3.** The two hexavalent ligands **13.3** and **7.15.3** showed approximately the same potency with IC_{50} = 37 μM and 33 μM, respectively. This suggests that, unlike the valency, the shape of the multivalent molecule may have a minor influence on the activity, at least in this type of assay. On the other hand, the PEG core of **7.15.3** may just be too flexible to modify the 3D structure of the dendrimer in a

significant way. The most remarkable improvement was observed in the case of the nonavalent system **9.15.3**, which, with a 15 μM IC_{50}, displays a RIP of 8.

The SPR competition assay results for all compounds of Figure 2 are shown in Figure 4 and the corresponding IC_{50} values are listed in Table 1. A gradual increase of activity was observed as a function of the scaffold valence increment for all ligands, except those derived from the pseudotrisaccharide **2,** that show RIP < 1 (Table 1, column 3). This unusual behavior of polyvalent materials derived form **2** was already observed for polyester dendrons[18] and is now confirmed to occur independently of the nature of the polyvalent support. More structural experiments are being carried out in our laboratory to analyze the factors that govern this phenomenon. Tethering mannose on tetravalent and hexavalent scaffolds afforded very minor improvements, but the affinity gradually increased with higher valence dendrimers, reaching an IC_{50} = 36 μM for the 18-valent construct **13.15.5** (RIP 5; Table 1, Entry 7, Man column). Comparing the activities of materials with different ligands, it is obvious that the selected lead **4** gives the best activity in the group. The tetravalent and hexavalent constructs **11.4** and **13.4** displayed a RIP of 6 and 9, respectively, leading to an IC_{50} = 6 μM for **13.4** (Table 1, Entry 3, column **4**). The threshold for water solubility of the nonavalent construct **9.15.4** was found to be at ca. 2 mg/mL (0.3 μM), which prevented the determination of activity curves. Nonetheless, the advantage of using a more powerful monovalent ligand in the preparation of multivalent constructs is obviously shown from these data (Figure 4): IC_{50} values in the low micromolar range are rapidly reached using the most powerful ligand **4** even in tetravalent presentation. Other mannosylated and pseudo-mannosylated materials lag behind, even when the sugar is presented with higher valency on the dendrimers.

*3.3 MD simulations of dendrimers **11** and **13***

In order to interpret the multivalency effect observed for the materials under study, it must be kept in mind that the SPR competition assay used here measures the ability of the dendrimers to inhibit binding of soluble DC-SIGN tetramers to an immobilized binding partner. Under these conditions, various effects can be operative. In principle, they may include 1) a high local concentration of the

ligand exposed by the dendrimers (or high effective molarity, which favors statistical rebinding;[34] 2) chelation, i.e. simultaneous binding of multiple binding sites by a single dendrimer on a single DC-SIGN tetramer, or 3) the ability of the dendrimers to cluster soluble DC-SIGN tetramers. [22] To gauge the average dimension of the most active dendrimers **11.4** and **13.4** and to estimate whether they can effectively span the distance between two DC-SIGN Ca^{2+} binding sites which are separated by approximately 4 nm, molecular dynamics simulations were employed. To speed up the calculations, the simulations were performed on models **11.3** and **13.3**, that ought to have the same size of the materials derived from **4**. Since mannose binds to DC-SIGN Ca^{2+} ions using O3 and O4, the distances between these atoms in different Man residues were monitored continuously during the dynamics, that were run for a total of 60 ns (details for **11.3** are collected in the Supplementary Information section). Results showed that, even at maximum extension, the distance between the two farthest Man-O3 is well below 4 nm (30.6 Å for **11.3** and 35.4 Å for **13.3**, Figure 5), so that chelation of two sites on the same DC-SIGN tetramer cannot be achieved. Hence, it is most likely that the modest multivalency effects measured for **11.4** and **13.4** result from increased effective molarity of the ligands and/or from an ability to cluster the soluble tetramers in the SPR experiments. In the real biological settings, where DC-SIGN is exposed on the surface of (dendritic) cells, this latter effect may be lost, or it may be translated into an ability to promote receptor clustering at the cell surface. Thus it is of interest to explore the activity of the dendrimers described here in cellular models of viral infections.

3.4 Infection tests

Tests were performed on both an HIV infection and a Dengue virus (DV) infection models.

DC-SIGN promotes HIV transmission by DCs to CD4+ T cells (infection in *trans*)[35]. For HIV studies, B-THP-1/DC-SIGN cells, that support DC-SIGN mediated HIV-1 transmission efficiently, were exploited as a model of DCs. The cells were pre-incubated for 30 minutes in the presence or absence of the DC-SIGN inhibitors and afterwards were pulsed with HIV-1 BaL in the continued presence of inhibitors. After washing, the B-THP-1/DC-SIGN cells were co-cultured with activated

CD4+ T lymphocytes from healthy volunteer donors. Viral infection of CD4+ T lymphocytes was monitored quantifying the concentration of the HIV-1 core protein p24 in the co-culture supernatants by ELISA. Mannan, a known DC-SIGN inhibitor[35-37] was used as a positive control. Non-transfected B-THP-1 cells, as expected, did not transmit infection. The HIV *trans* infection studies focused on those multivalent structures which were found to be the most active in the SPR experiment, namely dendrimers **11.4** and **13.4**, bearing 4 and 6 copies of the bisamide **4**. The results were compared to those obtained with **11.3** (tetravalent presentation of the pseudo-disaccharide **3**) to examine the effect of the monovalent ligand, and with the previously described tetravalent Boltorn-type dendron **1.2**. [1, 2](**Figure 6** and Supplementary **Figure SI-3)**.

Tetravalent **11.3** reduced the infection to 66% and 26% at 10 μM and 100 μM concentrations, respectively. After treatment with compound **11.4**, bearing four copies of **4**, 47% of infection was determined at 10 μM and almost no infection took place at 100 μM concentration. The most impressive inhibition of HIV *trans* infection was observed in the case of **13.4** (hexavalent **4**). At 1 μM concentration the infection was reduced to 50%, and at 10 μM and 100 μM the infection was completely suppressed. For comparison, the previously known tetravalent Boltorn-type pseudo-trisaccharide **1.2** showed similar activity to **11.4** (no infection at 100 μM) and was therefore clearly outperformed by **13.4**, which reduced the infection to 0% at 10-fold lower concentrations.

DC-SIGN also plays an important role during the transmission of Dengue virus and is considered as a target for therapeutics that block Dengue infection.[38, 39] Dengue infection is primarily transmitted by mosquitoes and the symptoms include fever, muscle and joint pains and skin rash. Methods for the control and prevention of Dengue by vaccination have not been established, yet [40]and previous attempts in our groups to block DC-SIGN mediated DV infections using mannosylated materials based on Boltorn scaffolds were unsuccessful. In order to examine the potential activity of the glycodendrimers to inhibit Dengue virus infection, Raji cells over-expressing DC-SIGN were infected with Dengue virus serotype-2 in the presence or absence of **13.4** at different concentrations, 10 μM, 5 μM and 1 μM (Figure 7). Gratifyingly, dendrimer **13.4**

showed concentration-dependent antiviral activity. At 10 μM concentration the infection was inhibited by about 85% and the IC_{50} was found to be 5.9 μM. The effect of **13.4** lasted even when the compound was removed 30 minutes after infection (Supplementary Information, Figure SI-7).

3.5 Discussion

A majority of pathogens that infect humans use the mucosal entry pathway. These pathogens include respiratory viruses and those responsible for sexually transmitted diseases including HIV and Human Papilloma Virus (HPV). Notably, mucosal infections continue to represent a challenge for the development of either preventive or therapeutic vaccines. A number of mucosal pathogens recognize DC-SIGN as their primary target. Therefore, the design of materials capable of interacting efficiently with DC-SIGN and of blocking the infections by pathogens that use this lectin to access the target cells is a topic of tremendous interest. Towards this goal, we have developed a strategy based on a very efficient click chemistry approach that allows to conjugate different carbohydrate and glycomimetic ligands to a variety of multimeric scaffolds with different valency. SPR competition studies have demonstrated that the dendrimers obtained bind efficiently to DC-SIGN with IC_{50}s in the μM range.

Among the materials synthesized, those based on the monovalent ligand **4** are the most interesting ones, since this ligand possesses the best selectivity observed to date for DC-SIGN versus Langerin, a critical issue for inhibiting HIV infection. These materials were also found to be the most active ones in the present study. The results showed that multivalent ligands functionalized with **4** can inhibit both HIV and Dengue virus at low micromolar range. In particular, the hexavalent dendrimer **13.4** exhibits a low μM range activity inhibiting *trans*-infection of T-cells by HIV in cellular studies and provides 100% inhibition of the infection at 10 μM concentration. The activity shown by **13.4** in the Dengue infection model is also very promising and it will be pursued further. Like HIV, Dengue virus is critically dependent on DC-SIGN for host infection. No clinical treatments are available for Dengue infection and there is a clear requirement for novel antiviral agents in this

field. Carbohydrate-based materials are under study as inhibitors of viral adsorption [40]. In our studies, the scaffold ligand combination provided by **13.4** is the only one that has proven effective to block DC-SIGN mediated uptake of DV. All previously tested dendrimers with mannose or **3** as a ligand were ineffective towards Dengue infection (not shown). Both the multivalent scaffold **13** and monovalent ligand **4** can be prepared in gram scale and only one CuAAC step is required to obtain the functionalized dendrimer **13.4**. Moreover, unlike the previously described multivalent compounds based on a polyester backbone, the final structure **13.4** is chemically stable. Thus **13.4** represents a clear step forward in the quest for effective antiviral therapeutics.

4. Conclusions

In summary, we present in this work the evolution of glycomimetic ligands of DC-SIGN in multivalent materials synthesized using very efficient click chemistry reactions. Their relative IC_{50} were determined with a SPR based test, allowing selection of compounds whose antiviral activity was tested using cellular models of infection with HIV and DV. The promising results obtained in these studies establish the bases for the preparation of improved materials with higher antiviral activities. Indeed, the studies performed here suggest that some improvement may still be obtained in avidity with scaffolds more apt to favor a chelating effect upon binding to DC-SIGN. It does not seem likely that such goal is already achieved with this first series of dendrimers that appear to act mostly through rebinding and clustering effects.

Acknowledgments. The project was supported under the EU ITN Marie-Curie program (CARMUSYS, Grant number 213592). The CM1102 COST Action Multiglyconano is also acknowledged. FF thanks the Institut Universitaire de France for financial support. A. Berzi was supported by a fellowship of University of Milan and Regione Lombardia (Programma “Dote Ricerca- Rafforzare il capitale umano”, POR-Ob.2 Asse IV-FSE 2007-2013). This work has been conducted thanks to the access to the SPR and MP3 platforms of the Partnership for Structural

Biology and the Institut de Biologie Structurale in Grenoble (PSB/IBS) . HRMS analysis were obtained at the CIGA center of the University of Milan.

References

[1] van Kooyk Y, Geijtenbeek TBH. DC-sign: Escape mechanism for pathogens. Nat Rev Immunol. 2003;3:697-709.

[2] Anderluh M, Jug G, Svajger U, Obermajer N. DC-SIGN Antagonists, a potential new class of anti-infectives. Curr Med Chem. 2012;19:992-1007.

[3] Date AA, Destache CJ. A review of nanotechnological approaches for the prophylaxis of HIV/AIDS. Biomaterials. 2013;34:6202-28.

[4] Borrok MJ, Kiessling LL. Non-carbohydrate inhibitors of the lectin DC-SIGN. J. AmChem Soc. 2007;129:12780-5.

[5] Garber KCA, Wangkanont K, Carlson EE, Kiessling LL. A general glycomimetic strategy yields non-carbohydrate inhibitors of DC-SIGN. Chem Commun. 2010;46:6747-9.

[6] Mangold SL, Prost LR, Kiessling LL. Quinoxalinone inhibitors of the lectin DC-SIGN. Chem Sci. 2012;3.

[7] Tran TH, El Baz R, Cuconati A, Arthos J, Jain P, Khan ZK. A novel high-throughput screening assay to identify inhibitors of HIV-1 gp120 protein interaction with DC-SIGN. J Antivir Antiretrovir. 2011;3:49-54.

[8] Lasala F, Arce E, Otero JR, Rojo J, Delgado R. Mannosyl glycodendritic structure inhibits DC-SIGN-mediated Ebola virus infection in cis and in trans. Antimicrob Agents Chemother. 2003;47:3970-2.

[9] Rojo J, Delgado R. Glycodendritic structures: promising new antiviral drugs. J Antimicrob Chemother. 2004;54:579-81.

[10] Bernardi A, Cheshev P. Interfering with the sugar code: design and synthesis of oligosaccharide mimics. Chemistry- Eur J. 2008;14:7434-41.

[11] de Witte L, Nabatov A, Pion M, Fluitsma D, de Jong MA, de Gruijl T, et al. Langerin is a natural barrier to HIV-1 transmission by Langerhans cells. Nat Med. 2007;13:367-71.

[12] Sattin S, Daghetti A, Thepaut M, Berzi A, Sanchez-Navarro M, Tabarani G, et al. Inhibition of DC-SIGN-mediated HIV infection by a linear trimannoside mimic in a tetravalent presentation. ACS Chem Biol. 2010;5:301-12.

[13] Berzi A, Reina JJ, Ottria R, Sutkeviciute I, Antonazzo P, Sanchez-Navarro M, et al. A glycomimetic compound inhibits DC-SIGN-mediated HIV infection in cellular and cervical explant models. AIDS. 2012;26:127-37.

[14] Thepaut M, Guzzi C, Sutkeviciute I, Sattin S, Ribeiro-Viana R, Varga N, et al. Structure of a glycomimetic ligand in the carbohydrate recognition domain of C-type lectin DC-SIGN. Structural requirements for selectivity and ligand design. J Am Chem Soc. 2013;135:2518-29.

[15] Varga N, Sutkeviciute I, Guzzi C, McGeagh J, Petit-Haertlein I, Gugliotta S, et al. Selective targeting of dendritic cell-specific intercellular adhesion molecule-3-grabbing nonintegrin (DC-SIGN) with mannose-based glycomimetics: synthesis and interaction studies of bis(benzylamide) derivatives of a pseudomannobioside. Chemistry-Eur J. 2013;19:4786-97.

[16] Cambi A, de Lange F, van Maarseveen NM, Nijhuis M, Joosten B, van Dijk EM, et al. Microdomains of the C-type lectin DC-SIGN are portals for virus entry into dendritic cells. J Cell Biol. 2004;164:145-55.

[17] de Bakker BI, de Lange F, Cambi A, Korterik JP, van Dijk EM, van Hulst NF, et al. Nanoscale organization of the pathogen receptor DC-SIGN mapped by single-molecule high-resolution fluorescence microscopy. Chemphyschem. 2007;8:1473-80.

[18] Luczkowiak J, Sattin S, Sutkeviciute I, Reina JJ, Sanchez-Navarro M, Thepaut M, et al. Pseudosaccharide functionalized dendrimers as potent inhibitors of DC-SIGN dependent Ebola pseudotyped viral infection. Bioconjug Chem. 2011;22:1354-65.

[19] Wang SK, Liang PH, Astronomo RD, Hsu TL, Hsieh SL, Burton DR, et al. Targeting the carbohydrates on HIV-1: interaction of oligomannose dendrons with human monoclonal antibody 2G12 and DC-SIGN. P Natl Acad Sci USA. 2008;105:3690-5.

[20] Becer CR, Gibson MI, Geng J, Ilyas R, Wallis R, Mitchell DA, et al. High-affinity glycopolymer binding to human DC-SIGN and disruption of DC-SIGN interactions with HIV envelope glycoprotein. J Am Chem Soc. 2010;132:15130-2.

[21] Martinez-Avila O, Bedoya LM, Marradi M, Clavel C, Alcami J, Penades S. Multivalent manno-glyconanoparticles inhibit DC-SIGN-mediated HIV-1 trans-infection of human T cells. Chembiochem. 2009;10:1806-9.

[22] Tabarani G, Reina JJ, Ebel C, Vives C, Lortat-Jacob H, Rojo J, et al. Mannose hyperbranched dendritic polymers interact with clustered organization of DC-SIGN and inhibit gp120 binding. FEBS Lett. 2006;580:2402-8.

[23] Arce E, Nieto PM, Diaz V, Castro RG, Bernad A, Rojo J. Glycodendritic structures based on Boltorn hyperbranched polymers and their interactions with Lens culinaris lectin. Bioconjug Chem. 2003;14:817-23.

[24] Maria S, Sanchez-Medina I, Mereghetti P, Belvisi L, Jimenez-Barbero J, Bernardi A. Synthesis and conformational analysis of an alpha-D-mannopyranosyl(1 -> 2)-alpha-D-mannopyranosyl-(1 -> 6)-alpha-D-mannopyranose mimic. Carbohydr Res. 2007;342:1859-68.

[25] Reina JJ, Sattin S, Invernizzi D, Mari S, Martinez-Prats L, Tabarani G, et al. 1,2-Mannobioside mimic: synthesis, DC-SIGN interaction by NMR and docking, and antiviral activity. ChemMedChem. 2007;2:1030-6.

[26] Canalle LA, van Berkel SS, de Haan LT, van Hest JCM. Copper-free clickable coatings. Adv Funct Mater. 2009;19:3464-70.

[27] Xie J, Hu L, Shi W, Deng X, Cao Z, Shen Q. Synthesis and nonlinear optical properties of hyperbranched polytriazole containing second-order nonlinear optical chromophore. J Polym Sci B Polym Phys. 2008;46:1140-8.

[28] Touaibia M, Wellens A, Shiao TC, Wang Q, Sirois S, Bouckaert J, et al. Mannosylated G(0) dendrimers with nanomolar affinities to Escherichia coli FimH. ChemMedChem. 2007;2:1190-201.

[29] Ortega-Munoz M, Lopez-Jaramillo J, Hernandez-Mateo F, Santoyo-Gonzalez F. Synthesis of glyco-silicas by Cu(I)-catalyzed "click-chemistry" and their applications in affinity chromatography. Adv Synth Catal. 2006;348:2410-20.

[30] Lambeth RH, Pederson SJ, Baranoski M, Rawlett AM. Methods for removal of residual catalyst from polymers prepared by ring opening metathesis polymerization. J Polym Sci A Polym Chem. 2010;48:5752-7.

[31] Tabarani G, Thepaut M, Stroebel D, Ebel C, Vives C, Vachette P, et al. DC-SIGN neck domain is a pH-sensor controlling oligomerization. SAXS and hydrodynamic studies of etracellular domain. J Biol Chem. 2009;284:21229-40.

[32] Huskens D, Vermeire K, Profy AT, Schols D. The candidate sulfonated microbicide, PRO 2000, has potential multiple mechanisms of action against HIV-1. Antiviral Res. 2009;84:38-47.

[33] Andreini M, Doknic D, Sutkeviciute I, Reina JJ, Duan JX, Chabrol E, et al. Second generation of fucose-based DC-SIGN ligands: affinity improvement and specificity versus Langerin. Org Biomol Chem. 2011;9:5778-86.

[34] Pieters RJ. Maximising multivalency effects in protein-carbohydrate interactions. Org Biomol Chem. 2009;7:2013-25.

[35] Geijtenbeek TBH, Torensma R, van Vliet SJ, van Duijnhoven GCF, Adema GJ, van Kooyk Y, et al. Identification of DC-SIGN, a novel dendritic cell-specific ICAM-3 receptor that supports primary immune responses. Cell. 2000;100:575-85.

[36] Hong PWP, Flummerfelt KB, de Parseval A, Gurney K, Elder JH, Lee B. Human immunodeficiency virus envelope (gp120) binding to DC-SIGN and primary dendritic cells is carbohydrate dependent but does not involve 2G12 or cyanovirin binding sites: Implications for structural analyses of gp120-DC-SIGN binding. J Virol. 2002;76:12855-65.

[37] Lin G, Simmons G, Pohlmann S, Baribaud F, Ni HP, Leslie GJ, et al. Differential N-linked glycosylation of human immunodeficiency virus and Ebola virus envelope glycoproteins modulates interactions with DC-SIGN and DC-SIGNR. J Virol. 2003;77:1337-46.

[38] Tassaneetrithep B, Burgess TH, Granelli-Piperno A, Trumpfherer C, Finke J, Sun W, et al. DC-SIGN (CD209) mediates dengue virus infection of human dendritic cells. J Exp Med. 2003;197:823-9.

[39] Lozach PY, Burleigh L, Staropoli I, Navarro-Sanchez E, Harriague J, Virelizier JL, et al. Dendritic cell-specific intercellular adhesion molecule 3-grabbing non-integrin (DC-SIGN)-mediated enhancement of dengue virus infection is independent of DC-SIGN internalization signals. J Biol Chem. 2005;280:23698-708.

[40] Hidari KI, Abe T, Suzuki T. Carbohydrate-related inhibitors of dengue virus entry. Viruses. 2013;5:605-18.

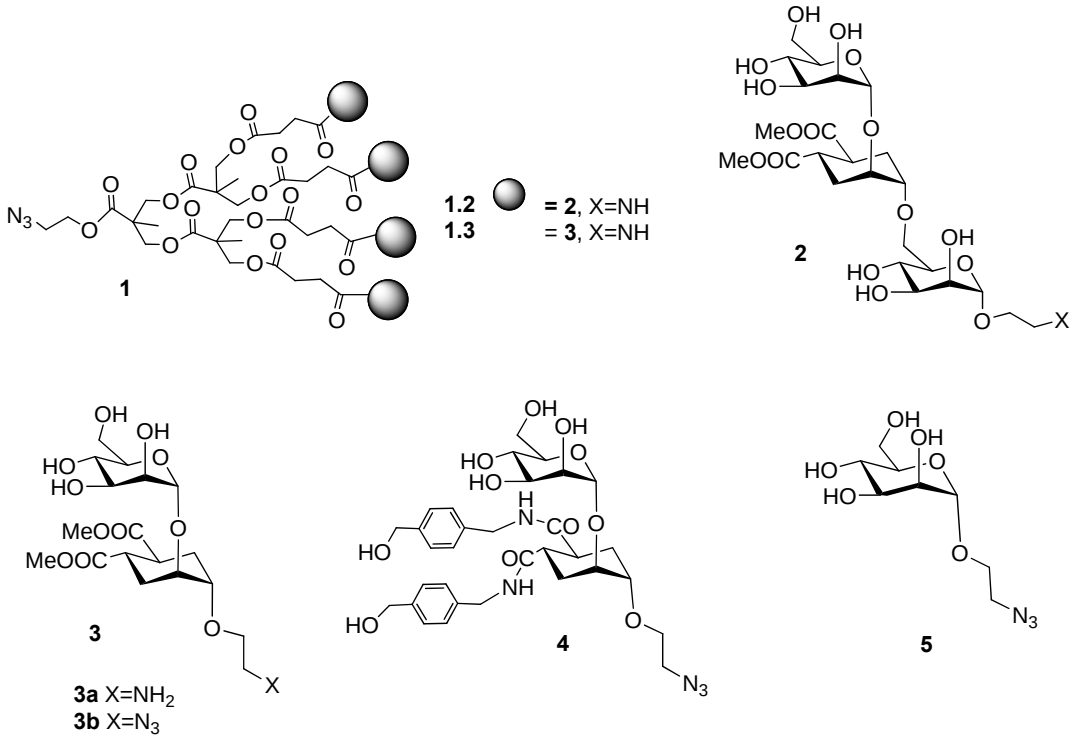

Figure 1. Monovalent glycomimetic ligands of DC-SIGN **2-5** and the tetravalent Boltorn-type dendron **1**

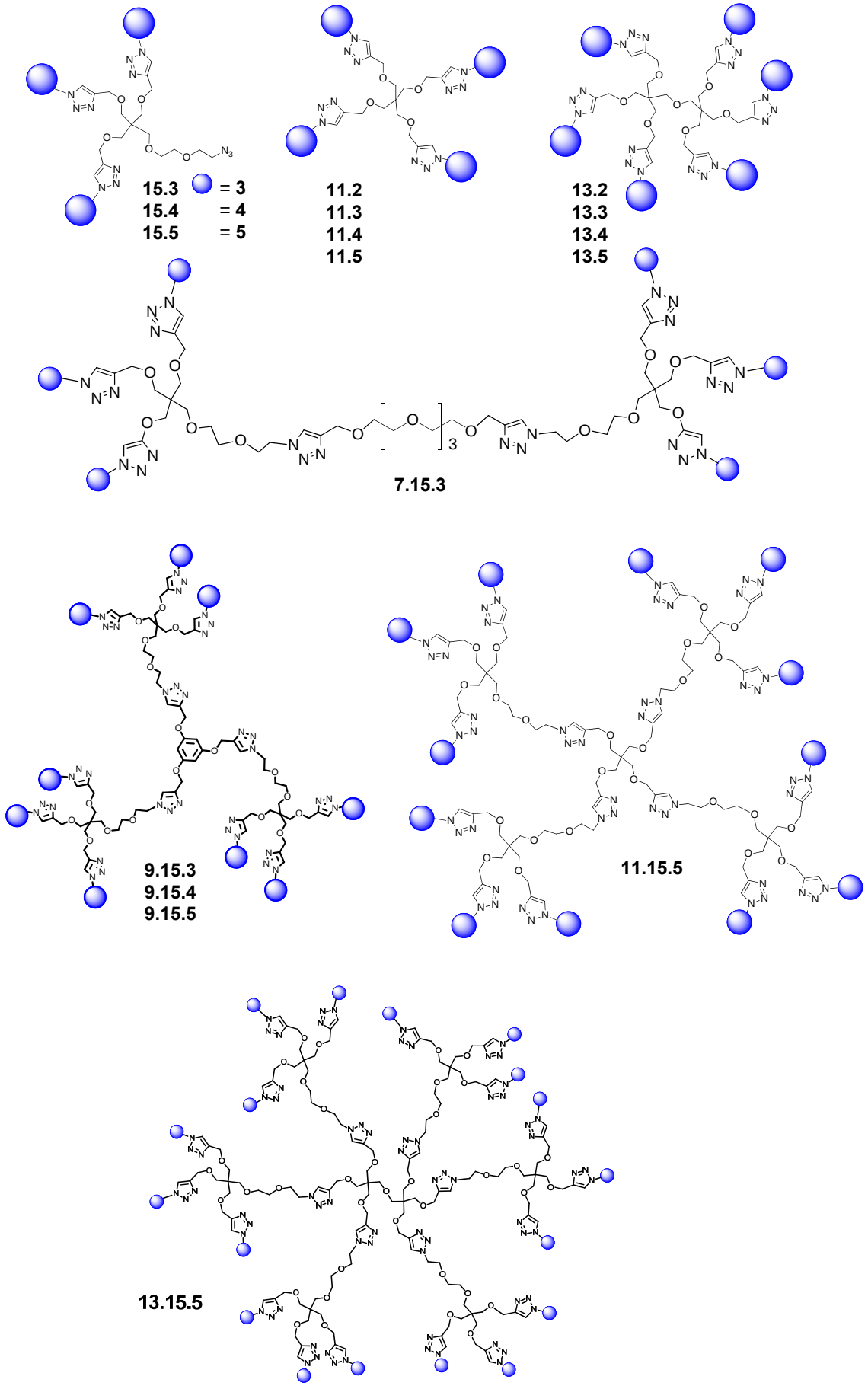

Figure 2. Dendrimers synthesized in this study.

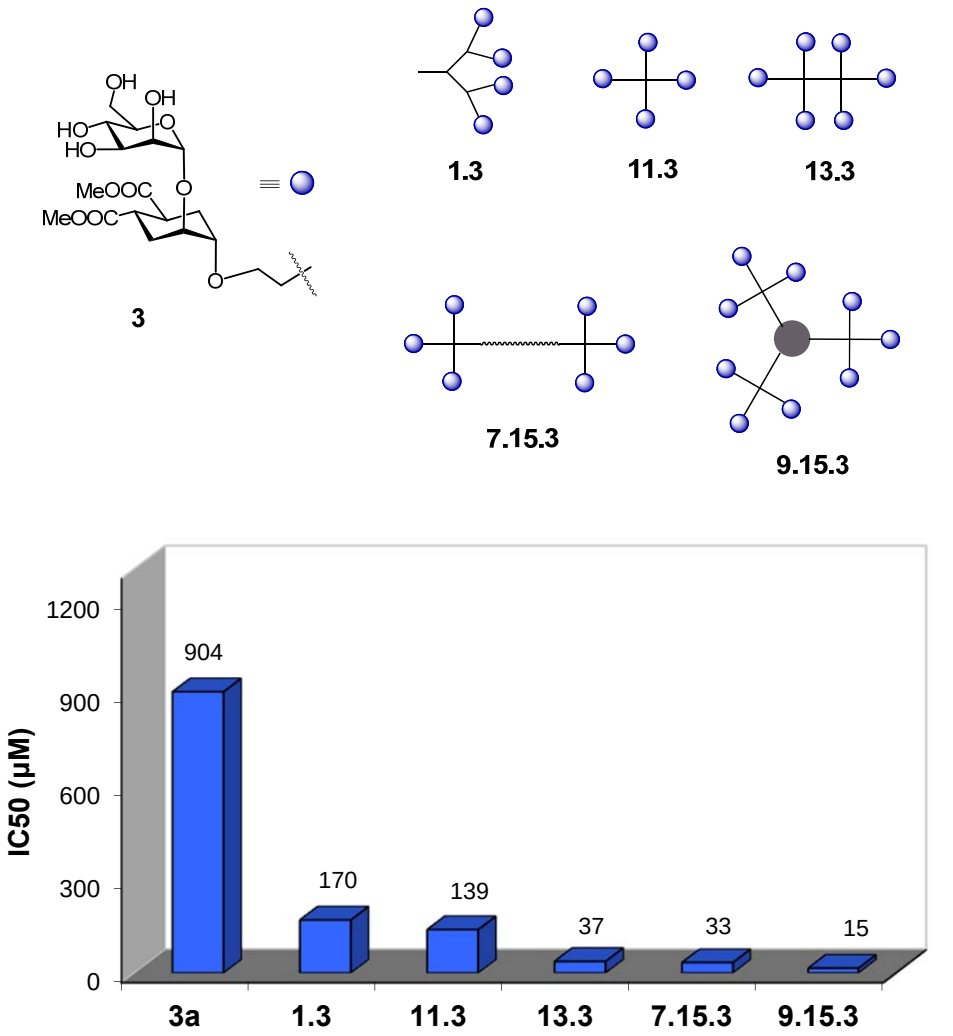

Figure 3. Schematic structures and IC_{50} values of the monovalent pseudo-disaccharide **3a**, glycodendron **1.3** (Boltorn type) and glycodendrimers **11.3**, **13.3**, **7.15.3** and **9.15.3** (pentaerythritol based) measured by SPR (competition experiments with immobilized Man-BSA)

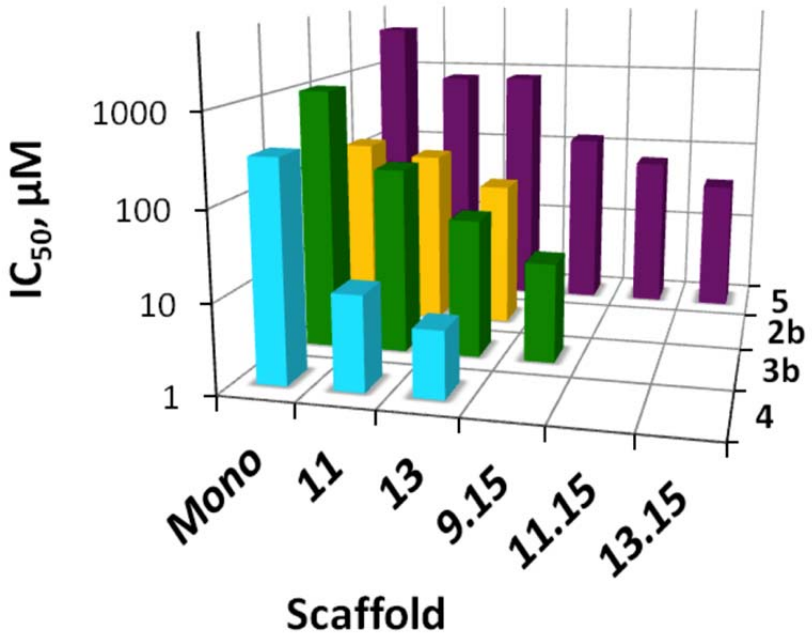

Figure 4. Comparison of the IC_{50} (µM) values obtained for similar dendrimers with different monovalent ligands (**2b, 3b, 4, 5**)

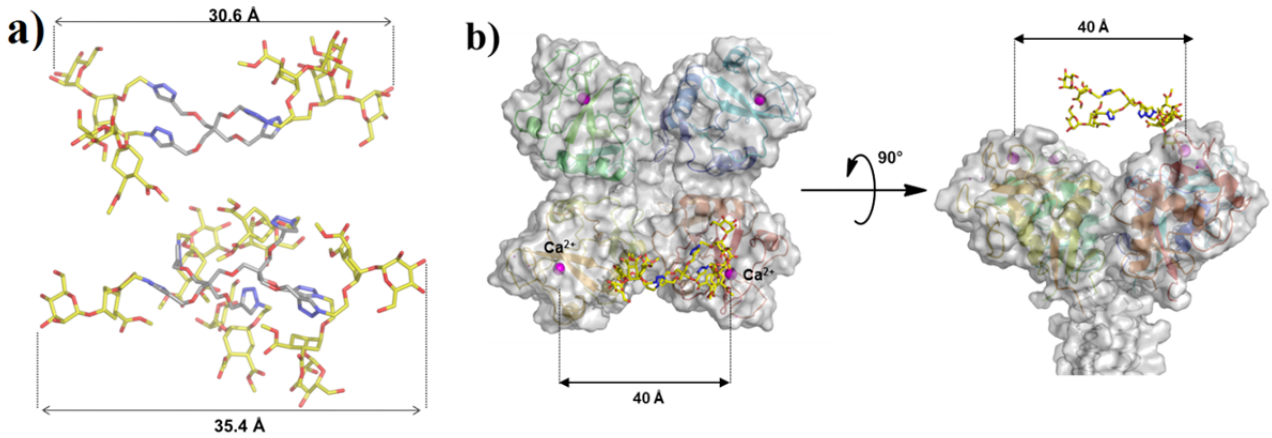

Figure 5. a) Extended structure of dendrimer **11.3** and **13.3;** b) Rigid docking of **11.3** (CPK model) in its extended structure on the DC-SIGN tetramer [31]

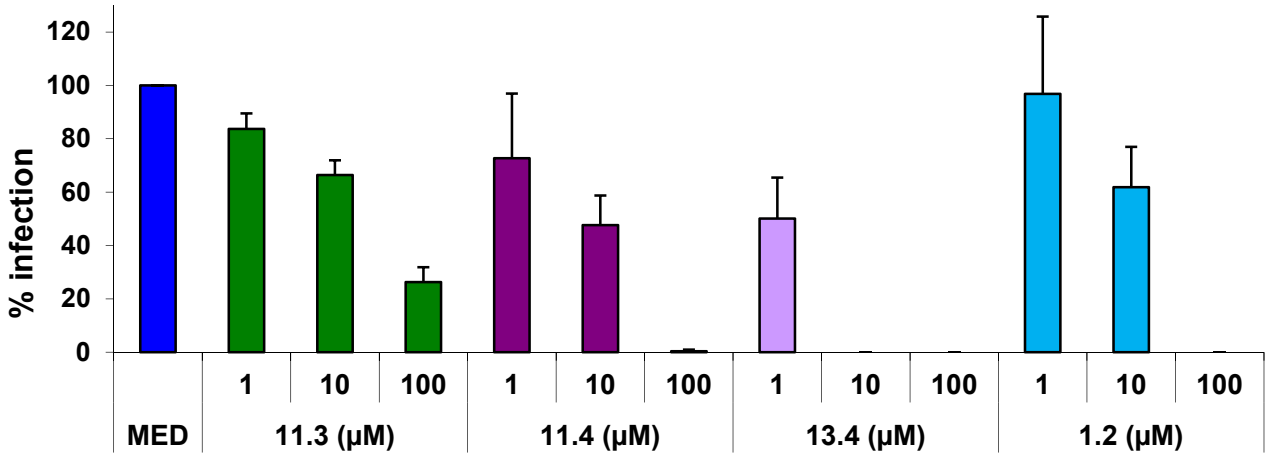

Figure 6. HIV *trans* infection levels after treatment with dendrimers (*trans* infection level measured as amount of p24 viral protein) Experiments were performed on CD4+ T cells purified from 3 healthy donors. Data are represented as percentage of untreated control infection level. Values represent the mean ±SD.

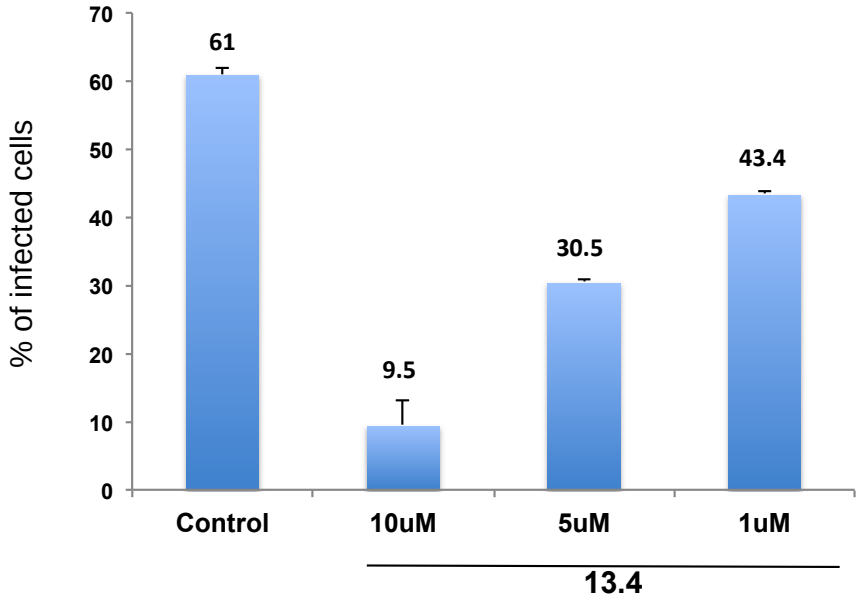

Figure 7. Dose dependent inhibition of DV infection by **13.4**. Raji-DCSIGN cells were infected with DV2 JAM at MOI-1 in the presence of **13.4** at different concentrations.

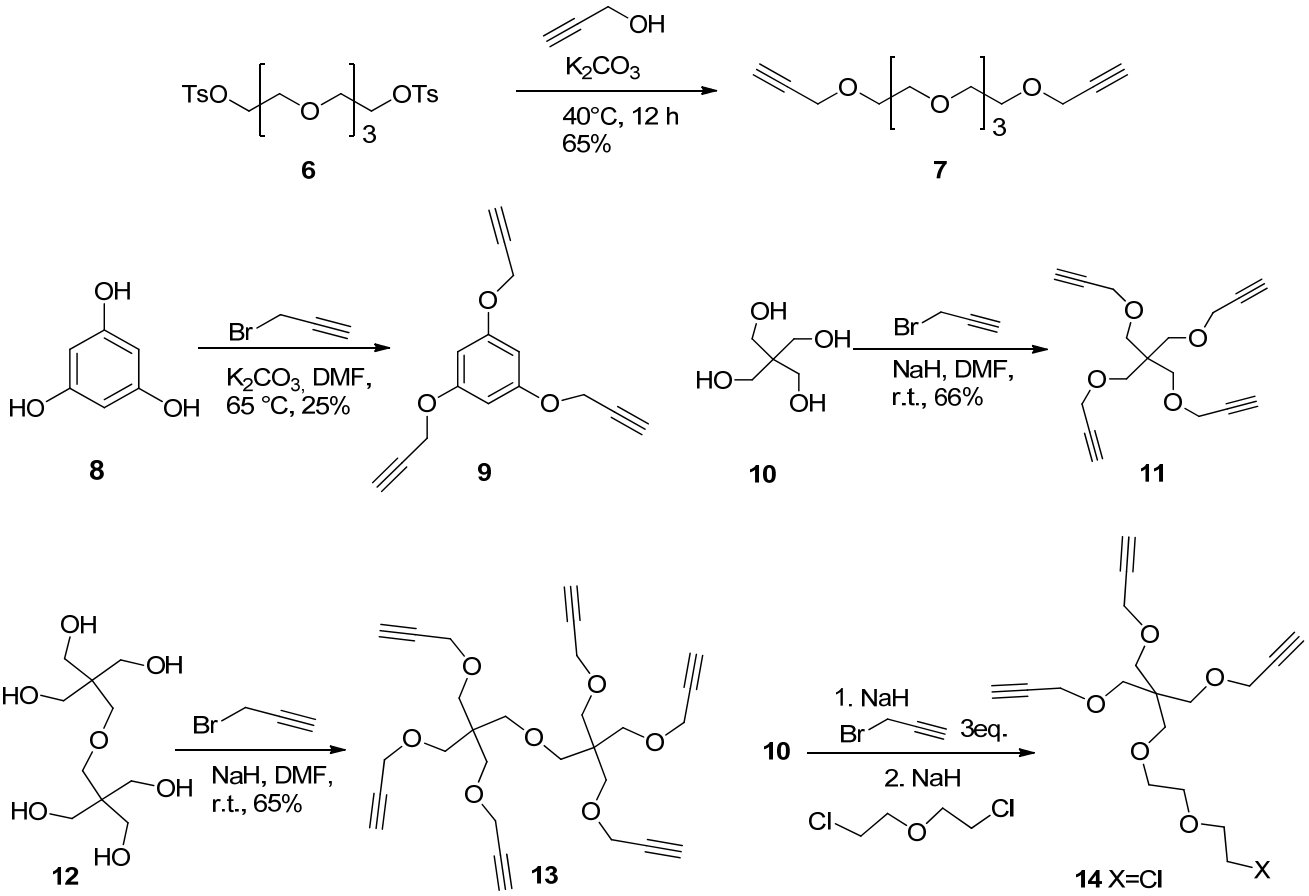

Scheme 1. Synthesis of the multivalent alkynes **7**, **9**, **11**, **13**, and **14**

Figure captions

Figure 1. Monovalent glycomimetic ligands of DC-SIGN 2-5 and the tetravalent Boltorn-type dendron **1**

Figure 2. Dendrimers synthesized in this study.

Figure 3. Schematic structures and IC_{50} values of the monovalent pseudo-disaccharide **3a**, glycodendron **1.3** (Boltorn type) and glycodendrimers **11.3**, **13.3**, **7.15.3** and **9.15.3** (pentaerythritol based) measured by SPR (competition experiments with immobilized Man-BSA)

Figure 4. Comparison of the IC_{50} (μM) values obtained for similar dendrimers with different monovalent ligands (**2b, 3b, 4, 5**)

Figure 5. a) Extended structure of dendrimer 11.3 and 13.3; b) Rigid docking of 11.3 (CPK model) in its extended structure on the DC-SIGN tetramer [31]

Figure 6. HIV *trans* infection levels after treatment with dendrimers (*trans* infection level measured as amount of p24 viral protein) Experiments were performed on CD4+ T cells purified from 3 healthy donors. Data are represented as percentage of untreated control infection level. Values represent the mean ±SD.

Figure 7. Dose dependent inhibition of DV infection by **13.4**. Raji-DCSIGN cells were infected with DV2 JAM at MOI-1 in the presence of **13.4** at different concentrations.

Scheme 1. Synthesis of the multivalent alkynes **7**, **9**, **11**, **13**, and **14**

Table 1. $IC_{50} \pm$ SD values (μM) obtained in DC-SIGN inhibition assays (SPR)

			Ligand		
Entry	**Valency**	**5** (cmpd numb., RIP[a])	**2** (cmpd numb., RIP[a])	**3** (cmpd numb., RIP[a])	**4** (cmpd numb., RIP[a])
1	1	3292 ± 337 (**5**, 1)	145 ± 83 (**2**, 1)	1018 ± 109 (**3b**, 1)	308 ± 40 (**4**, 1)
2	4	767 ± 20 (**11.5**, 1.1)	112 (**11.2,** 0.3)	136 ± 23 (**11.3**, 1.9)	12± 3 (**11.4**, 6.4)
3	6	800 (**13.5**, 0.7)	51 (**13.2**, 0.5)	39 (**13.3**, 4)	5.7 ± 1.6 (**13.4**, 9)
4	6	-	-	32 (**7.15.3**, 5)	
5	9	128 (**9.15.5**, 2.8)	-	14 (**9.15.3**, 8)	-[b]
6	12	67 (**11.15.5**, 4.1)	-	-	-
7	18	36 (**13.15.5**, 5.1)	-	-	-

a) Relative Inhibitory Potency, calculated as $(IC_{50})_{mono}/IC_{50*}$valency ;
b) Not measured, due to the low water solubility of **9.15.4**